Optical Materials 36 (2014) 611–615

Contents lists available at ScienceDirect

Optical Materials

journal homepage: www.elsevier.com/locate/optmat

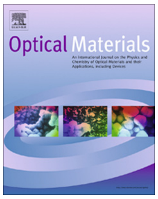

Realization of tunable emission via efficient Tb^{3+}–Eu^{3+} energy transfer in $K_3Gd(PO_4)_2$ for UV-excited white light-emitting-diodes

Tingming Jiang [a], Xue Yu [a,b], Xuhui Xu [a,b], Hongling Yu [a], Dacheng Zhou [a,b], Jianbei Qiu [a,b,*]

[a] College of Materials Science and Engineering, Kunming University of Science and Technology, Kunming 650093, PR China
[b] Key Laboratory of Advanced Materials of Yunnan Province, Kunming 650093, PR China

ARTICLE INFO

Article history:
Received 13 July 2013
Received in revised form 12 October 2013
Accepted 29 October 2013
Available online 22 November 2013

Keywords:
Energy transfer
Phosphors
Orange-yellow
w-LEDs

ABSTRACT

A n-UV convertible phosphor $K_3Gd(PO_4)_2$:Tb^{3+}, Eu^{3+} with tunable-emitting color has been synthesized by the solid state reaction. Under the Tb^{3+} excitation (373 nm), the Eu^{3+} emissions increase dramatically with increasing the Eu^{3+} content due to the efficient energy transfer from Tb^{3+} to Eu^{3+}, which has been justified through the luminescence spectra and fluorescence decay curves. $K_3Gd(PO_4)_2$:$0.5Tb^{3+}$, yEu^{3+} can achieve tunable color emissions from yellowish-green through orange-yellow and ultimately to reddish-orange by simply adjusting the Eu^{3+} content. In addition, the energy transfer mechanism was demonstrated to be the dipole–dipole interaction and the energy transfer efficiency was calculated. The present results indicate that this novel orange-yellow emitting phosphor can be as a potential candidate for the application in white LEDs.

1. Introduction

White light emitting diodes (LED) have been paid more and more attention due to their high efficiency, low voltage, long service life, mercury pollution-free, and energy conversation [1–4]. Currently, commercial white LEDs are fabricated by combing InGaN blue chips with yellow emitting phosphors. Especially, yellow phosphors have attracted great attention since they make it possible to easily fabricate white LEDs with low cost, high brightness, and long life time [5]. At present, $Y_3Al_5O_{12}$:Ce^{3+} (YAG:Ce^{3+}) yellow phosphor is the most frequently applied to obtain white LEDs. However, YAG:Ce^{3+} provides an unsatisfactory high correlated color temperature ($Tc > 4500$ K) and low color rendering indexes ($Ra < 80$) for general illumination due to the lack of red emission in the spectra [6,7]. Another approach may solve this problem by using a near UV-LED chip (350–420 nm) coated with blue-green and orange emitting phosphors to generate warm with light. This method offers white LEDs with excellent color rendering indexes and low correlated color temperatures [8,9]. Therefore, much attention has focused on developing orange-yellow emitting phosphors which has more red emission component than YAG:Ce^{3+}. So far, several such phosphors based on nitride or oxynitride have been studied [10–12]. However, compared with oxide-type phosphors, most nitride and oxynitride-type phosphors suffer from harsh preparation conditions, such as high-temperature nitrification at high pressure or carbothermal reaction [13]. Therefore, it is necessary to research oxide-type orange-yellow emitting phosphors using comparatively simple synthesis approaches for UV-excited wLEDs.

Recently, increasing attention has been focused on the development luminescence materials based on phosphate hosts due to their low sintering temperature, high luminous efficiency, and high stability [14–16]. To the best of our knowledge, there are very few reports on Eu^{3+}/Tb^{3+} co-doped $K_3Gd(PO_4)_2$ materials for potential applications in white LEDs. In this work, we report a new orange-yellow emitting phosphate-type phosphor: $K_3Gd(PO_4)_2$:Tb^{3+}, Eu^{3+}, which was prepared by the conventional solid-state method. The color emission of this novel phosphor can be easily tuned from yellowish-green to reddish-orange by adjusting the Eu^{3+} concentration. The efficient energy transfer from Tb^{3+} to Eu^{3+} in $K_3Gd(PO_4)_2$ was investigated systematically.

2. Experimental sections

The $K_3Gd(PO_4)_2$:Tb^{3+}, Eu^{3+} phosphors were synthesized by conventional solid-state method. Analytical reagent grade K_2CO_3, Gd_2O_3, TbF_3, Eu_2O_3, $NH_4H_2PO_4$ were employed as raw materials, which were weighed out and mixed homogeneously by an agate mortar for 30 min and placed in an alumina crucible. This crucible was heated at 950 °C for 6 h under air atmosphere and slowly cooled to room temperature.

The phases of the obtained samples were identified by X-ray powder diffraction (XRD) with Cu Kα ($\lambda = 1.5418$ Å) radiation at a

---

* Corresponding author at: College of Materials Science and Engineering, Kunming University of Science and Technology, Kunming 650093, PR China. Tel./fax: +86 8715188856.

E-mail address: qiu@kmust.edu.cn (J. Qiu).

0925-3467/$ - see front matter © 2013 Elsevier B.V. All rights reserved.
http://dx.doi.org/10.1016/j.optmat.2013.10.039

scanning step of 0.02° in the 2θ range from 10° to 90°, operated at 36 kV and 30 mA (Rigaku Model D/max-2200). The photoluminescence (PL) and photoluminescence excitation (PLE) spectra were measured with a HITACHI F-7000 fluorescence spectrophotometer, using a static 150 W Xe lamp as the excitation source. The fluorescence decay curves were measured by Jobin Yvon FL3 fluorescence spectrophotometer. All the measurements were carried out at room temperature.

3. Results and discussions

Fig. 1 shows the X-ray diffraction patterns of the $K_3Gd(PO_4)_2$:Tb^{3+}, Eu^{3+} phosphors. The XRD patterns of as-prepared $K_3Gd(PO_4)_2$ compounds accompanying with different doping rare earth ions are in good agreement with the reported $K_3Gd(PO_4)_2$ phase (JCPDS card No. 49-1085), indicating all samples are of single phase. The crystal structure of $K_3Gd(PO_4)_2$ belongs to the monoclinic crystal system with space group P 2_1/m ($Z = 2$). The basic structural units are composed of isolated GdO_7 decahedron and PO_4 tetrahedron. Every GdO_7 decahedron is connected with six PO_4 tetrahedron to form two dimension $Gd(PO_4)2^{3-}$ sheets in the *a*–*b* plane. The K atoms are inserted along the *c*-axis between these sheets [17]. According to the effective ionic radii of cations with different coordination number reported by Shannon [18], The ionic radii of Gd^{3+} for seven-coordinated is 1.00 Å, and the ionic radii of Tb^{3+}, Eu^{3+} for seven-coordinated are 0.98, 1.01 Å. In addition, there are three different K^+ sites which coordination numbers are 9, 10, 11 and the radii of them are 1.55 Å, 1.59 Å, 1.64 Å respectively. Evidently, they are too big for Tb^{3+} and Eu^{3+} to occupy. Therefore, for the consideration of ionic radii matching, these Tb^{3+} and Eu^{3+} ions should substitute for the Gd^{3+} sites in the $K_3Gd(PO_4)_2$ host.

Fig. 2a shows the PLE and PL spectra of $K_3Gd(PO_4)_2$:$0.5Tb^{3+}$. The broad band at 200–300 nm is corresponding to the spin-allow transition from the 4f to the 5d state of Tb^{3+} ion, whereas the sharp lines in the range of 300–400 nm are ascribed to excitation due to the forbidden f–f transition of Tb^{3+} ion [19]. The line located at about 273 nm is attributed to the $^8S_{7/2}$–^6I_J transition of Gd^{3+} [20]. The PL spectrum shows the characteristic sharp emission lines centered at 485, 542, 580, and 619 nm corresponding to transitions from $^5D_4$ level to the $^7F_6$, $^7F_5$, $^7F_4$, and $^7F_3$ levels of Tb^{3+} [21]. However, emissions in the blue region that come from the high energy of the $^5D_3$ level cannot be observed. As the $^5D_3$–$^5D_4$ transition is resonant with the $^7F_6$–$^7F_0$ transition, the emissions of $^5D_3$–^7F_J transitions are often quenched for high Tb^{3+} concentration doped samples due to the cross relaxation $^5D_3 + {}^7F_6 \rightarrow {}^5D_4 + {}^7F_0$ [22].

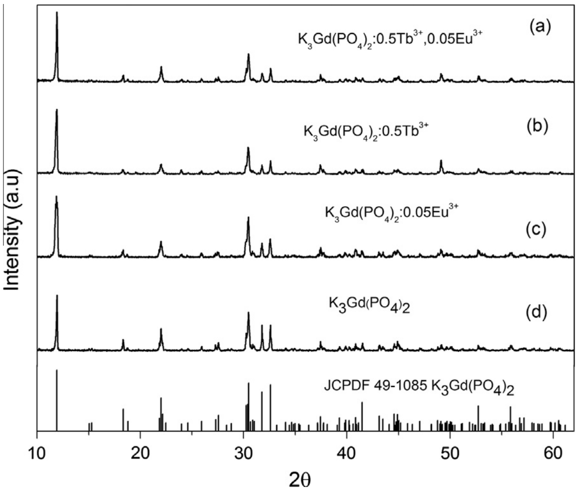

Fig. 1. XRD patterns of $K_3Gd(PO_4)_2$ (a) $K_3Gd(PO_4)_2$:$0.05Eu^{3+}$ (b) $K_3Gd(PO_4)_2$:$0.5Tb^{3+}$ (c) $K_3Gd(PO_4)_2$:Tb^{3+}, Eu^{3+} (d) The standard data for $K_3Gd(PO_4)_2$ (JCPDS card No. 49-1085) is shown as a reference.

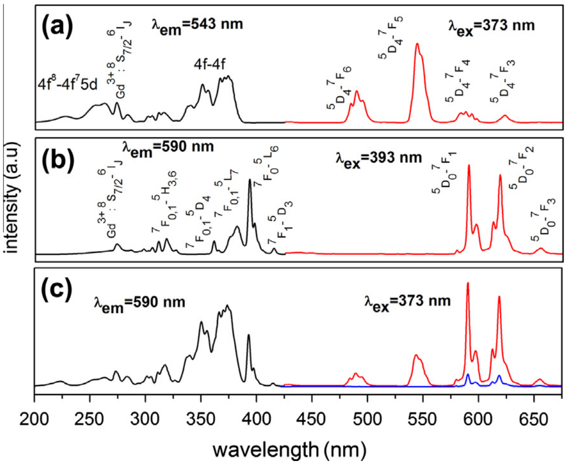

Fig. 2. PLE (left) and PL (right) spectra of $K_3Gd(PO_4)_2$:$0.5Tb^{3+}$ (a), $K_3Gd(PO_4)_2$:$0.05Eu^{3+}$ (b) and $K_3Gd(PO_4)_2$:$0.5Tb^{3+}$,$0.05Eu^{3+}$ (c).

Fig. 2b presents the PLE and PL spectra of $K_3Gd(PO_4)_2$:$0.05Eu^{3+}$. The excitation spectrum by monitoring 590 nm contains a group of sharp peaks located at 318 nm ($^7F_{0,1}$–$^5H_{3,6}$), 360 nm ($^7F_{0,1}$–$^5D_4$), 380 nm ($^7F_{0,1}$–$^5L_7$), 392 nm ($^7F_{0,1}$–$^5L_6$), 413 nm ($^7F_{0,1}$–$^5D_3$) [23], respectively. The peak at 273 nm is also assigned to $^8S_{7/2}$–^6I_J transition of Gd^{3+}. The emission spectrum exhibits characteristic sharp peaks of Eu^{3+} located at 580, 590, 618 and 653 nm which are corresponding to $^5D_0$–$^7F_0$, $^5D_0$–$^7F_1$, $^5D_0$–$^7F_2$, $^5D_0$–$^7F_3$ transitions [23], respectively. In Fig. 2c, the black line shows the PLE spectrum by monitoring 590 nm for $K_3Gd(PO_4)_2$:$0.5Tb^{3+}$,$0.05Eu^{3+}$. The red line presents the PL spectrum of $K_3Gd(PO_4)_2$:$0.5Tb^{3+}$,$0.05Eu^{3+}$ under 373 nm. And the blue line shows the PL spectrum of $K_3Gd(PO_4)_2$:$0.05Eu^{3+}$ under 373 nm. It is obvious to observe that the excitation spectrum of $K_3Gd(PO_4)_2$:$0.5Tb^{3+}$,$0.05Eu^{3+}$ has large differences with that of $K_3Gd(PO_4)_2$:$0.05Eu^{3+}$ by monitoring 590 nm, the 4f–4f transitions of Tb^{3+} can be observed and dominate the excitation spectrum except for the f–f transitions of Eu^{3+}. This observation may relate to the efficient Tb^{3+}–Eu^{3+} energy transfer because of the incorporation of highly amount of Tb^{3+} ions into $K_3Gd(PO_4)_2$:Eu^{3+}. The emission spectra directly verify the sensitization of Eu^{3+} luminescence by Tb^{3+}–Eu^{3+} energy transfer. Under excitation of Tb^{3+} (373 nm), the PL spectrum of $K_3Gd(PO_4)_2$:$0.05Eu^{3+}$ (blue line) shows very weak emissions of Eu^{3+} located at 590 and 613 nm. However, the red line (PL spectrum of $K_3Gd(PO_4)_2$:$0.5Tb^{3+}$,$0.05Eu^{3+}$) shows emissions from both Tb^{3+} and Eu^{3+}, and the emission intensities from Eu^{3+} (590, 613 nm) are much stronger than those of Tb^{3+} (485, 542 nm), verifying that Eu^{3+} can be excited efficiently by the excitation of Tb^{3+} when the Tb^{3+} ions were introduced into $K_3Gd(PO_4)_2$:Eu^{3+} samples.

In order to further investigate the energy transfer process between the Tb^{3+} and Eu^{3+} ions in $K_3Gd(PO_4)_2$ host, a serials of samples were synthesized. Fig. 3 shows the PL spectra for Tb^{3+} and Eu^{3+} co-doped $K_3Gd(PO_4)_2$:$0.5Tb^{3+}$, yEu^{3+} ($y = 0$, 0.005, 0.01, 0.03, 0.05, 0.07, 0.1, 0.15) phosphors. Under excitation with 373 nm UV light, the characteristic sharp emissions of Tb^{3+} as well as sharp emission peaks of Eu^{3+} are observed in emission spectra. The emission intensities of Tb^{3+} at 488, 544 nm decreased remarkably with increasing Eu^{3+} concentration which is assigned to the enhancement of energy transfer from Tb^{3+} to Eu^{3+}; whereas the emission intensities of Eu^{3+} at 590, 613 nm increased initially and reaches a maximum at $y = 0.1$, beyond which it decreases because the energy transfer efficiency from Tb^{3+} to Eu^{3+} is close to saturation with increasing the Eu^{3+} concentration. The critical distance R_c for energy transfer